Scientia Iranica F (2021) 28(3), 1917–1925

SCIENTIA IRANICA

Sharif University of Technology
Scientia Iranica
Transactions F: Nanotechnology
http://scientiairanica.sharif.edu

Entropy generation optimization and activation energy in flow of Walters-B nanomaterial

S. Jabeen[a,*], T. Hayat[a,b], and A. Alsaedi[b]

a. *Department of Mathematics, Quaid-I-Azam University 45320, Islamabad 44000, Pakistan.*
b. *Department of Mathematics, Faculty of Science, King Abdulaziz University, Jeddah 21589, Saudi Arabia.*

Received 7 October 2019; received in revised form 24 September 2020; accepted 26 October 2020

KEYWORDS
Viscous dissipation; Walters-B nanofluid; Entropy generation; Thermal radiation; Heat generation/absorption; Activation energy.

Abstract. The present study addresses the entropy generation in the flow of Walters-B nanomaterial. Energy equation consists of ohmic heating, radiation, and heat generation. Binary chemical reaction with the modified Arrhenius energy was employed in this study. In addition, the consequences of thermophoresis, Brownian motion, and viscous dissipation were taken into account. Convergent solutions were presented using homotopy analysis. Intervals of convergence were explicitly identified. The results of physical quantities of interest were analyzed. There was a decrease in the mass transfer rate at a higher value of chemical reaction parameter. Enhanced values of Brinkman number and magnetic parameter caused a decrease in the total entropy rate.

1. Introduction

Extensive applications of nanotechnology to thermal engineering have given rise to a new branch of heat transfer fluids called nanofluids. In nanofluid formation, fibers, solid particles, and tubes (with a length of order 1–50 nm) are dispersed in heat transfer materials like oil, water, and ethylene glycol. These materials are considered as the base fluids owing to their small size and mostly, the larger surface area of particles. The nanofluids are characterized by novel properties including higher thermal conductivity, negligible blockage in flow channels, homogeneity, and log-term constancy. Nanofluids are employed in many fields including microelectronics, automotive, power stations, fuel chambers, pharmacological methods, hybrid electric engines, cooling engine automobile, caloric controlling, local refrigerator, crushing process, mining and boiler gas outlet, temperature control, and nuclear process. Nanomaterials benefit from a special auditory characteristic that is easy to use in ultrasonic demonstration. Additional function of nanomaterials includes shear transformation of an instant compression ray which becomes more operatable with an increase in its concentration. Information of rheological implementation of nanofluids is more influential in view of their stability for convection applications. Pioneering work on nanofluid was done by Choi [1]. Recently Waini et al. [2] studied the hybrid nanomaterial flow and heat mechanism over a nonlinear porous surface. Some studies for flow of nanofluids can be consulted through the attempts [3–11].

In thermodynamics, entropy of any system is defined as the quantity of inaccessible energy. It corresponds to the irreversibility of the studied system and is mainly used in thermodynamical design setups. Higher entropy loss leads to greater energy consumption and negatively affects the system efficiency. Entropy rep-

*. *Corresponding author. Tel.: + 92 51 90642172*
E-mail address: sumaira.jabeen@math.qau.edu.pk (S. Jabeen)

doi: 10.24200/sci.2020.54593.3822

resents a procedure by which physical quantities are easily separated from the constituents. Upon supplying thermal energy to the system, one can notice internal energy increase; as a result, the thermal entropy of the system is enhanced. Irreversible processes are defined as the systems in which the surroundings of the related system would not be able to reach their initial state. Entropy is also related to the consumption of energy in a system. System changes occur mostly due to gradients.

Temperature gradient represents energy transfer or may be a concentration gradient that indicates mass transfer. Gradient mostly causes irreversibility within a system. Entropy relates to the disorderedness of the system due to which energy decreases and consequently, reduces the potential for operation. Bejan has conducted a pioneering work on this phenomenon [12]. Later on, he discussed entropy generation in the process of heat loss during fluid motion [13]. Several researchers have lately analyzed this mechanism under certain assumptions. Recently Liu et al. [14] examined irreversibility within a curved channel in Electro Magnetohydrodynamics (EMHD) flow. Dissipative flow of Williamson fluid by rotating disk with entropy generation is analyzed by Qayyum et al. [15]. Akbarzadeh et al. [16] explained irreversibility in turbulent nanofluid flow by considering solar stoves through crenelated absorber plates. Bizhaem and Abbassi [17] deliberated heat exchange and irreversibility in flow in a helical tube. Recent progresses about this topic can be listed in the form of academic attempts [18–21].

The main theme of this present research is to address entropy generation and activation energy in flow of nanomaterial. Constitutive expression of Walter-B liquid is employed in modeling. Joule heating, radiation, and heat generation/absorption in energy expression are present. Total entropy rate and Bejan number are formulated. The modeled mathematical problems are computed for the convergent series solution. Homotopic procedure [22–35] is adopted for developing solutions. Discussion and conclusions are organized for physical quantities of interest against the sundry variables entering into the present analysis.

2. Modeling

Here, this study addresses the irreversibility process and activation energy with a binary chemical reaction in the flow of Walters-B nanomaterial bounded by a stretching surface. An incompressible liquid is analyzed in the presence of magnetic field with constant strength B_0. Small magnetic Reynolds number leads to the omission of induced magnetic field. Here, x and y-axes are parallel and normal to the surface. Heat source/sink is considered. Surface temperature and concentration are taken as $\tilde{T}_w$ and $\tilde{C}_w$, while ambient

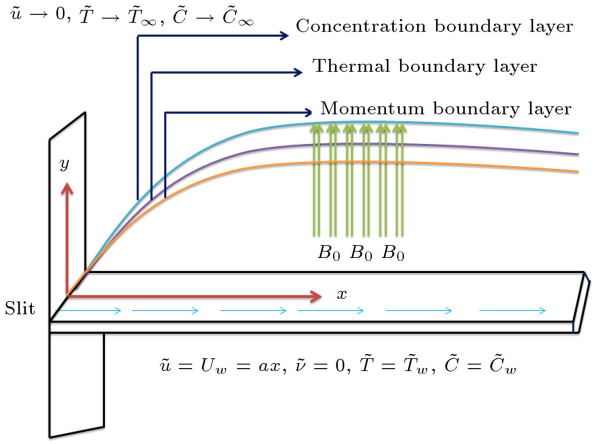

Figure 1. Flow geometry.

temperature and concentration are respectively denoted by $\tilde{T}_\infty$ and $\tilde{C}_\infty$. Figure 1 describes the problem geometry. The governing mathematical equations of the system are given below [8,26,32]:

$$\frac{\partial \tilde{u}}{\partial x} + \frac{\partial \tilde{v}}{\partial y} = 0, \tag{1}$$

$$\tilde{u}\frac{\partial \tilde{u}}{\partial x} + \tilde{v}\frac{\partial \tilde{u}}{\partial y} = \upsilon\frac{\partial^2 \tilde{u}}{\partial y^2} - \frac{k_0}{\rho}\left(\tilde{u}\frac{\partial^3 \tilde{u}}{\partial x \partial y^2} + \frac{\partial \tilde{u}}{\partial x}\frac{\partial^2 \tilde{u}}{\partial y^2} + \tilde{v}\frac{\partial^3 \tilde{u}}{\partial y^3} - \frac{\partial \tilde{u}}{\partial y}\frac{\partial^2 \tilde{u}}{\partial x \partial y}\right) - \frac{\tilde{\sigma} B_0^2}{\rho}\tilde{u}, \tag{2}$$

$$\tilde{u}\frac{\partial \tilde{T}}{\partial x} + \tilde{v}\frac{\partial \tilde{T}}{\partial y} = \frac{k}{\rho c_p}\frac{\partial^2 \tilde{T}}{\partial y^2} + \frac{\mu}{\rho c_p}\left(\frac{\partial \tilde{u}}{\partial y}\right)^2 - \frac{k_0}{\rho c_p}\left[\frac{\partial \tilde{u}}{\partial x}\left(\frac{\partial \tilde{u}}{\partial y}\right)^2 + \tilde{u}\frac{\partial \tilde{u}}{\partial y}\frac{\partial^2 \tilde{u}}{\partial x \partial y} + \tilde{v}\frac{\partial \tilde{u}}{\partial y}\frac{\partial^2 \tilde{u}}{\partial y^2} + 2\left(\frac{\partial \tilde{u}}{\partial y}\right)^2\frac{\partial \tilde{v}}{\partial y}\right] + \frac{1}{\rho c_p}\frac{16\sigma^* \tilde{T}_\infty^3}{3k^*}\frac{\partial^2 \tilde{T}}{\partial y^2} + \frac{Q_0}{\rho c_p}(\tilde{T} - \tilde{T}_\infty) + \tau\left[D_B\frac{\partial \tilde{T}}{\partial y}\frac{\partial C}{\partial y} + \frac{D_{\tilde{T}}}{\tilde{T}_\infty}\left(\frac{\partial \tilde{T}}{\partial y}\right)^2\right], \tag{3}$$

$$\tilde{u}\frac{\partial \tilde{C}}{\partial x} + \tilde{v}\frac{\partial \tilde{C}}{\partial y} = D_B\left(\frac{\partial^2 \tilde{C}}{\partial y^2}\right) + \frac{D_{\tilde{T}}}{\tilde{T}_\infty}\left(\frac{\partial^2 \tilde{T}}{\partial y^2}\right) - K_r^2(\tilde{C} - \tilde{C}_\infty)\left[\frac{\tilde{T}}{\tilde{T}_\infty}\right]^n \exp\left[\frac{-E_a}{k_1 \tilde{T}}\right], \tag{4}$$

subject to the conditions:

$$\tilde{u} = U_w = ax,\ \tilde{v} = 0,\ \tilde{T} = \tilde{T}_w,\ \tilde{C} = \tilde{C}_w \quad \text{at} \quad y = 0$$

$$\tilde{u} \to 0, \quad \tilde{T} \to \tilde{T}_\infty \quad \tilde{C} \to \tilde{C}_\infty \quad \text{as} \quad y \to \infty. \tag{5}$$

Here, (u, v) are velocity components in (x, y) directions, (k_0), (k), (c_p), (ρ), $(\tilde{\sigma})$, (σ^*), (k^*), (Q_0), (D_B), (K_r), (E_a), (k_1), and $(D_{\tilde{T}})$ denote material constant, density, electrical conductivity, specific heat, thermal conductivity, Stefan-Boltzmann constant, mean absorption coefficient, heat generation coefficient, Brownian diffusion coefficient, Boltzmann constant, dimensionless constant, or rate constant having the range $-1 < n < 1$, chemical reaction parameter, activation energy, and thermophoretic diffusion coefficient, respectively.

$$\psi = \sqrt{av}x\overset{\vee}{f}(\eta), \qquad \eta = \sqrt{\frac{a}{v}}y,$$

$$\overset{\vee}{\theta}(\eta) = \frac{\tilde{T} - \tilde{T}_\infty}{\tilde{T}_w - \tilde{T}_\infty}, \qquad \overset{\vee}{\phi}(\eta) = \frac{\tilde{C} - \tilde{C}_\infty}{\tilde{C}_w - \tilde{C}_\infty}. \tag{6}$$

Employing these transformation gives:

$$\overset{\vee}{f}''' - \overset{\vee}{f}'^2 + \overset{\vee}{f}\overset{\vee}{f}'' - K_0(2\overset{\vee}{f}'\overset{\vee}{f}'''' - \overset{\vee}{f}\overset{\vee}{f}'''' - \overset{\vee}{f}''^2) - M\overset{\vee}{f}' = 0, \tag{7}$$

$$(1+R)\overset{\vee}{\theta}'' + \Pr\ Ec\left[K_0\overset{\vee}{f}\overset{\vee}{f}''\overset{\vee}{f}''' + (\overset{\vee}{f}''^2)\right] + \Pr N_b\overset{\vee}{\theta}'\overset{\vee}{\phi}' + \Pr N_t(\overset{\vee}{\theta}')^2 + \Pr\ \tilde{Q}\overset{\vee}{\theta} = 0, \tag{8}$$

$$\overset{\vee}{\phi}'' + \frac{N_t}{N_b}\overset{\vee}{\theta}'' + \Pr Le\overset{\vee}{f}\overset{\vee}{\phi}' - \Pr Le\tilde{A}^2(1+\tilde{\delta}\overset{\vee}{\theta})^n \exp\left[\frac{-\overset{\circ}{E}}{1+\tilde{\delta}\overset{\vee}{\theta}}\right]\overset{\vee}{\phi} = 0, \tag{9}$$

$$\overset{\vee}{f}'(\eta) = 1, \quad \overset{\vee}{f}(\eta) = 0, \quad \overset{\vee}{\theta}(\eta) = 1, \quad \overset{\vee}{\phi}(\eta) = 1;$$

$$\text{at} \quad \eta = 0,$$

$$\overset{\vee}{f}'(\eta) \to 0, \quad \overset{\vee}{\theta}(\eta) \to 0, \quad \overset{\vee}{\phi}(\eta) \to 0;$$

$$\text{at} \quad \eta \to \infty, \tag{10}$$

where:

$$K_0 = \frac{k_0 a}{\mu},\ M = \frac{\tilde{\sigma}B_0^2}{\rho a},\ R = \frac{16\sigma^*\tilde{T}_\infty^3}{3kk^*},\ \Pr = \frac{\mu c_p}{k},$$

$$\text{Ec} = \frac{U_w^2}{c_p(T_w - T_\infty)}, \quad N_b = \frac{(\rho c)_p D_B(C_w - C_\infty)}{v(\rho c)_f},$$

$$N_t = \frac{(\rho c)_p D_T(T_w - T_\infty)}{v(\rho c)_f}, \quad \tilde{Q} = \frac{Q_0}{a\rho c_p},$$

$$Le = \frac{(k/\rho c_p)}{D_B}, \quad \overset{\circ}{E} = \frac{-E_a}{k_1\tilde{T}_\infty}, \quad \tilde{\delta} = \frac{(\tilde{T}_w - \tilde{T}_\infty)}{\tilde{T}_\infty},$$

$$\tilde{A} = \frac{K_r^2}{a}. \tag{11}$$

In the above expressions, the definitions (M), $(\Pr)$, (N_t), (Le), (R), (Ec), $(\tilde{Q})$, (N_b), (K_0), $(\overset{\circ}{E})$, $(\tilde{\delta})$, and $(\tilde{A})$ denote magnetic parameter, Prandtl number, thermophoresis parameter, Lewis number, radiation parameter, Eckert number, heat generation variable, Brownian motion parameter, non-dimensional fluid parameter, dimensionless activation energy parameter, temperature ratio parameter, and non-dimensional chemical reaction parameter, respectively.

Coefficient of skin friction and Nusselt and Sherwood numbers are reflected in the definitions given below:

$$\tilde{C}_{fx} = \frac{2\,\tilde{\tau}_w|_{y=0}}{\rho U_w^2}, \tag{12}$$

$$\tilde{N}_{ux} = \frac{x\,\tilde{q}_w|_{y=0}}{k(\tilde{T}_w - \tilde{T}_\infty)}, \tag{13}$$

$$\tilde{S}_{hx} = \frac{x\,\tilde{q}_m|_{y=0}}{D_B(\tilde{C}_w - \tilde{C}_\infty)}, \tag{14}$$

where:

$$\tilde{\tau}_w = \mu\frac{\partial u}{\partial y} - k_0\left(u\frac{\partial^2 u}{\partial x \partial y} - 2\frac{\partial u}{\partial x}\frac{\partial u}{\partial y}\right), \tag{15}$$

$$\tilde{q}_w = k\frac{\partial \tilde{T}}{\partial y} + \frac{16\sigma^*\tilde{T}_\infty^3}{3k^*}\frac{\partial \tilde{T}}{\partial y}, \tag{16}$$

$$\tilde{q}_m = D_B\frac{\partial \tilde{C}}{\partial y}. \tag{17}$$

Eqs. (6) and (12)–(17) give:

$$\text{Re}_x^{0.5}\tilde{C}_{fx} = 2[1 + K_0\overset{\vee}{f}'(0)]\overset{\vee}{f}''(0), \tag{18}$$

$$\text{Re}_x^{-0.5}\tilde{N}_{ux} = -\left(1 + \frac{4}{3}R\right)\overset{\vee}{\theta}'(0), \tag{19}$$

$$\text{Re}_x^{-0.5}\tilde{S}_{hx} = -\overset{\vee}{\phi}'(0), \tag{20}$$

where $\text{Re}_x = \frac{xU_w}{v}$ is the local Reynold's number.

3. Entropy generation examination

Irreversibility analysis for nanofluid flow of Walter's-B fluid with Arrhenius activation energy is conducted here. Thermal radiation, viscous dissipation, and Magnetohydrodynamics (MHD) effects are considered in entropy generation minimization. The corresponding dimensional form under the mentioned effects is given

below:

$$\left.\begin{aligned}\tilde{S}'''_{gen} =& \underbrace{\frac{k}{\tilde{T}^2}\left[1+\frac{16\sigma^*\tilde{T}_\infty^3}{3kk^*}\right]\left(\frac{\partial\tilde{T}}{\partial y}\right)^2}_{\text{heat transfer irreversibility}} \\ &+ \underbrace{\frac{1}{\tilde{T}}\tilde{\Phi}}_{\text{viscous dissipation irreversibility}} \\ &+ \underbrace{\frac{\sigma B_0^2 \breve{u}^2}{\tilde{T}}}_{\text{Joule heating irreversibility}} \\ &+ \underbrace{\frac{RD}{\tilde{C}_\infty}\left(\frac{\partial\tilde{C}}{\partial y}\right)^2+\frac{RD}{\tilde{T}_\infty}\left(\frac{\partial\tilde{T}}{\partial y}\right)\left(\frac{\partial\tilde{C}}{\partial y}\right)}_{\text{diffusive irreversibility}}\end{aligned}\right\} \quad (21)$$

$$\begin{aligned}\tilde{\Phi} =& k_0\left[\frac{\partial u}{\partial x}\left(\frac{\partial u}{\partial y}\right)^2+u\frac{\partial u}{\partial y}\frac{\partial^2 u}{\partial x\partial y}+v\frac{\partial u}{\partial y}\frac{\partial^2 u}{\partial y^2}\right. \\ &\left.+2\left(\frac{\partial u}{\partial y}\right)^2\frac{\partial v}{\partial y}\right], \quad (22)\end{aligned}$$

Substituting Eq. (22) into Eq. (21), we get:

$$\left.\begin{aligned}\tilde{S}'''_{gen} =& \underbrace{\frac{k}{\tilde{T}^2}\left[1+\frac{16\sigma^*\tilde{T}_\infty^3}{3kk^*}\right]\left(\frac{\partial\tilde{T}}{\partial y}\right)^2}_{\text{heat transfer irreversibility}} \\ &+ \underbrace{\frac{k_0}{\tilde{T}}\left[\frac{\partial u}{\partial x}\left(\frac{\partial u}{\partial y}\right)^2+u\frac{\partial u}{\partial y}\frac{\partial^2 u}{\partial x\partial y}+v\frac{\partial u}{\partial y}\frac{\partial^2 u}{\partial y^2}+2\left(\frac{\partial u}{\partial y}\right)^2\frac{\partial v}{\partial y}\right]}_{\text{viscous dissipation irreversibility}} \\ &+ \underbrace{\frac{RD}{\tilde{C}_\infty}\left(\frac{\partial\tilde{C}}{\partial y}\right)^2+\frac{RD}{\tilde{T}_\infty}\left(\frac{\partial\tilde{T}}{\partial y}\right)\left(\frac{\partial\tilde{C}}{\partial y}\right)}_{\text{diffusive irreversibility}} \\ &+ \underbrace{\frac{\sigma B_0^2 \breve{u}^2}{\tilde{T}}}_{\text{Joule heating irreversibility}}.\end{aligned}\right\} \quad (23)$$

Upon employing transformations, the entropy minimization becomes:

$$\begin{aligned}N_G =& (1+R)\mathrm{Re}\,\overset{\vee}{\theta}'^2+\frac{K_0 BrRe}{\Omega_1}\overset{\vee}{f}\overset{\vee}{f}''\overset{\vee}{f}''' \\ &+\mathrm{Re}\lambda_1\left(\frac{\xi}{\Omega_1}\right)^2\overset{\vee}{\phi}'^2 \\ &+\mathrm{Re}\lambda\frac{\xi}{\Omega_1}\overset{\vee}{\theta}'\overset{\vee}{\phi}'+\frac{\mathrm{Re}MBr}{\Omega_1}\overset{\vee}{f}'^2, \quad (24)\end{aligned}$$

$$\mathrm{Br}=\frac{\mu U_w^2}{k\Delta\tilde{T}}, \quad \Omega_1=\frac{\Delta\tilde{T}}{\tilde{T}_\infty}, \quad \lambda_1=\frac{RD\tilde{C}_\infty}{k},$$

$$\xi=\frac{\Delta\tilde{C}}{\tilde{C}_\infty}, \quad N_G=\frac{S'''_G\tilde{T}_\infty x^2}{k\left(\Delta\tilde{T}\right)^2}, \quad (25)$$

where (N_G), (λ_1), (Br), (ξ), and (Ω) denote total entropy rate, diffusion constant, Brinkman number, concentration, and temperature difference parameters, respectively.

4. Solution methodology

Series solution of the above-mentioned system is obtained via homotopic technique. The suitable initial iterations $(\overset{\vee}{f}_0, \overset{\vee}{\theta}_0, \overset{\vee}{\phi}_0)$ and the corresponding linear operators $(\tilde{\mathcal{L}}_{\overset{\vee}{f}}, \tilde{\mathcal{L}}_{\overset{\vee}{\theta}}, \tilde{\mathcal{L}}_{\overset{\vee}{\phi}})$ are given below:

$$\overset{\vee}{f}_0(\eta)=1-e^{\eta}, \quad \overset{\vee}{\theta}_0(\eta)=e^{-\eta}, \quad \overset{\vee}{\phi}_0(\eta)=e^{-\eta}, \quad (26)$$

$$\tilde{\mathcal{L}}_{\overset{\vee}{f}}(\eta)=\frac{d^3\overset{\vee}{f}}{d\eta^3}-\frac{d\overset{\vee}{f}}{d\eta}, \quad \tilde{\mathcal{L}}_{\overset{\vee}{\theta}}(\eta)=\frac{d^2\overset{\vee}{\theta}}{d\eta^2}-\overset{\vee}{\theta},$$

$$\tilde{\mathcal{L}}_{\overset{\vee}{\phi}}(\eta)=\frac{d^2\overset{\vee}{\phi}}{d\eta^2}-\overset{\vee}{\phi}, \quad (27)$$

$$\tilde{\mathcal{L}}_{\overset{\vee}{f}}\left[\hat{X}_1+\hat{X}_2e^{\eta}+\hat{X}_3e^{-\eta}\right]=0, \quad (28)$$

$$\tilde{\mathcal{L}}_{\overset{\vee}{\theta}}\left[\hat{X}_4e^{\eta}+\hat{X}_5e^{-\eta}\right]=0, \quad (29)$$

$$\tilde{\mathcal{L}}_{\overset{\vee}{\phi}}\left[\hat{X}_6e^{\eta}+\hat{X}_7e^{-\eta}\right]=0. \quad (30)$$

where $\hat{X}_i(i=1-7)$ are termed as arbitrary constants.

5. Convergence analysis

To conduct the convergence analysis, the $\hbar$-curves are displayed in Figure 2. It is noticed that the series solutions converge in a range of auxiliary parameters that satisfy, $-1.5 \leq \hbar_f \leq -0.5$, $-1.4 \leq \hbar_\theta \leq -0.6$, and $-1.8 \leq \hbar_\phi \leq -0.4$. Numerical values of convergent solution are displayed in Table 1. Clearly, the momentum equation converges at the 9th order of approximation, while the 15th and 19th orders of approximations are enough for temperature and concentration. A comparison between the reduced Nusselt number $(\mathrm{Re}_x^{-0.5}\tilde{N}_{ux})$ and the published result is given in Table 2.

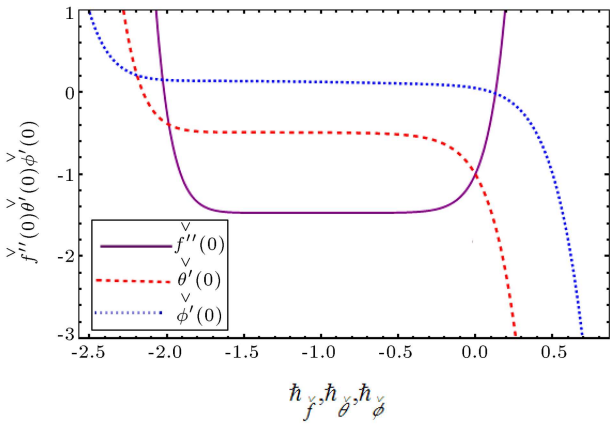

Figure 2. $\hbar$-curves for $\hbar_f$, $\hbar_\theta$, and $\hbar_\varphi$.

Table 1. Convergence table for velocity, temperature, and concentration when $M = 0.3$, $\Pr = 1.2$, $N_t = 0.4 = Le$, $R = 0.7 = \text{Ec}$, $\tilde{Q} = 0.3$, $N_b = 0.25 = K_0$, $\overset{\circ}{E} = 0.9 = \tilde{\delta}$, and $\tilde{A} = 0.65$.

Order of approximations	$-\overset{\vee}{f}''(0)$	$-\overset{\vee}{\theta}'(0)$	$\overset{\vee}{\phi}'(0)$
1	1.3500	0.73167	0.077040
9	1.4719	0.49925	0.11297
15	1.4719	0.49195	0.12603
19	1.4719	0.49195	0.12967
30	1.4719	0.49195	0.12967
40	1.4719	0.49195	0.12967

Table 2. Code verification for $\text{Re}_x^{-0.5}\tilde{N}_{ux}$, when $R = 0 = K_0$ for values of $\overset{\circ}{E}$ and $\tilde{A}$.

$\overset{\circ}{E}$	$\tilde{A}$	Mustafa et al. [10]	Present
0	1	0.9412	0.9412
1	–	1.0139	1.0139
2	–	1.0645	1.0645
4	–	1.1145	1.1145
1	0	1.1453	1.1453
1	1	1.0139	1.0139
–	2	0.9262	0.9262
–	5	0.7986	0.7986

6. Discussion

Figures (3–20) show the velocity, temperature, concentration, and entropy generation minimization in view of involved parameters. Figure 3 presents the outcome of (M) on velocity. For $(M = 0.1, 0.3, 0.5, 0.7)$, the velocity decays gradually when Lorentz fore (opposing force) is enhanced. In Figure 4, change in velocity is shown at higher values of dimensionless fluid parameter (K_0). An increase in $(K_0 = 0.5, 0.6, 0.7, 0.8)$ yields a reduction in velocity.

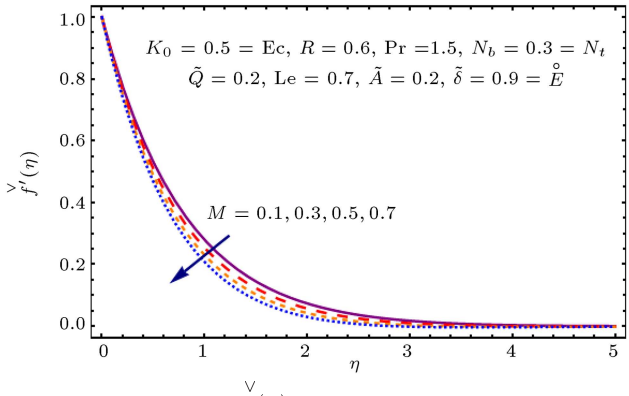

Figure 3. Impact on $\overset{\vee}{f}(\eta)$ via M.

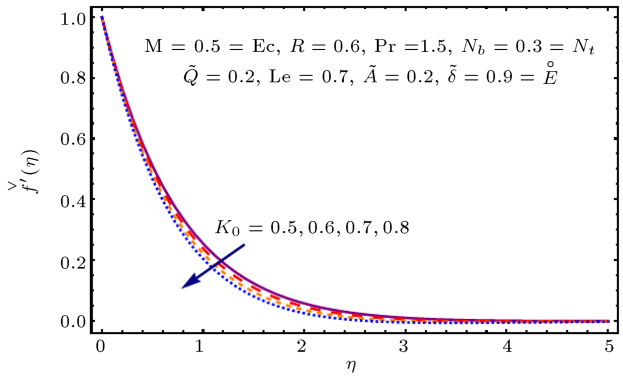

Figure 4. Impact on $\overset{\vee}{f}(\eta)$ via K_0.

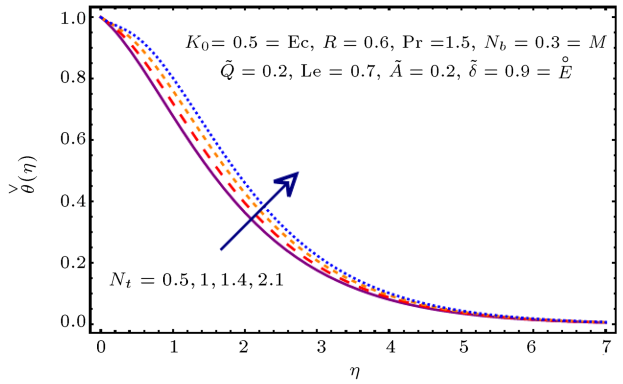

Figure 5. Impact on $\overset{\vee}{\theta}(\eta)$ via N_t.

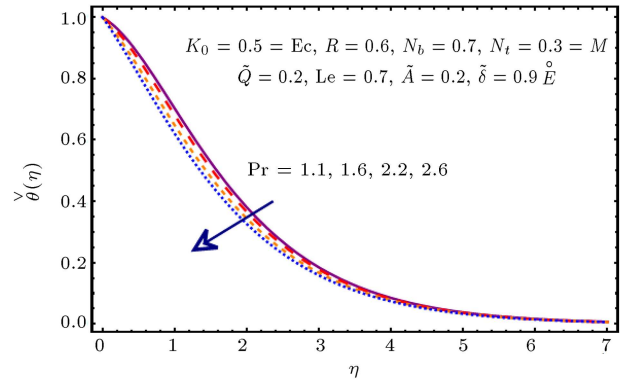

Figure 6. Impact on $\overset{\vee}{\theta}(\eta)$ via Pr.

Temperature for N_t variation is shown in Figure 5. Temperature is enhanced for $(N_t = 0.5, 1, 1.4, 2.1)$. Heat transfer occurs from a hotter region to a cooler one. This process boosts the temperature. Variation of (Pr) with respect to temperature is shown in Figure 6. Thermal diffusivity decays for (Pr = 1.1, 1.6, 2.2, 2.6) and temperature decreases. Figure 7 shows the outcome of Eckert number with respect to temperature. Temperature is an increasing function of (Ec = 0.5, 0.9, 1.3, 1.6). Higher Eckert number gives rise to the kinetic energy of fluid and consequently, fluid temperature is enhanced. Figure 8 provides a description of

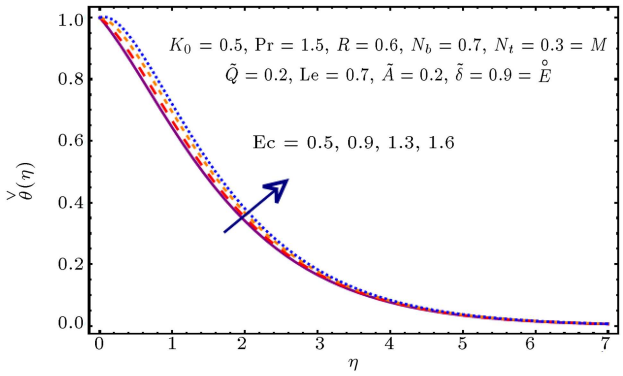

Figure 7. Impact on $\breve{\theta}(\eta)$ via Ec.

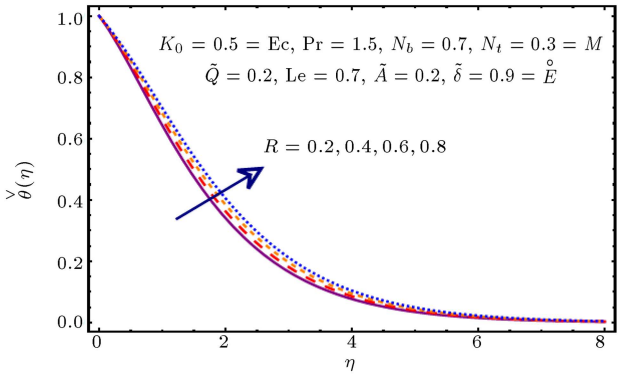

Figure 8. Impact on $\breve{\theta}(\eta)$ via R.

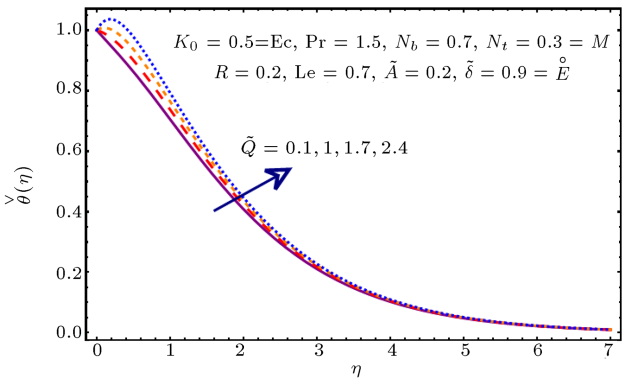

Figure 9. Impact on $\breve{\theta}(\eta)$ via $\tilde{Q}$.

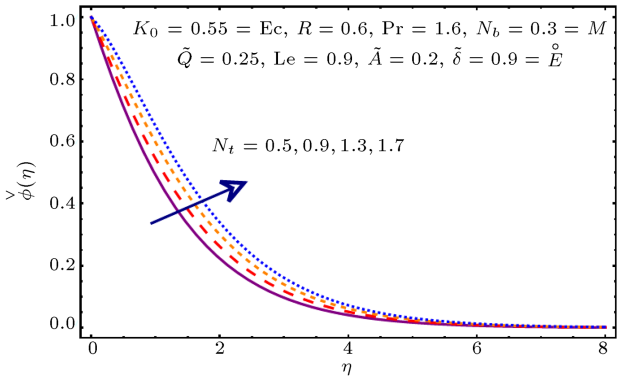

Figure 10. Impact on $\breve{\varphi}(\eta)$ via N_t.

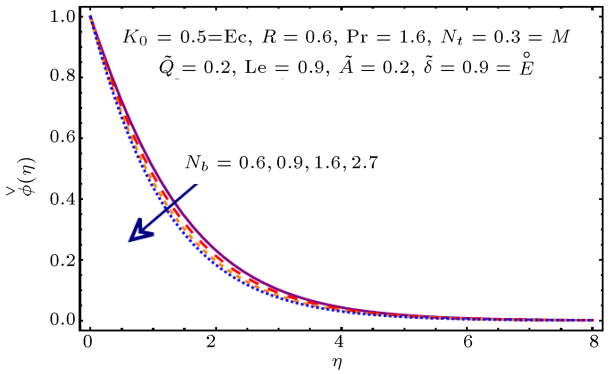

Figure 11. Impact on $\breve{\varphi}(\eta)$ via N_b.

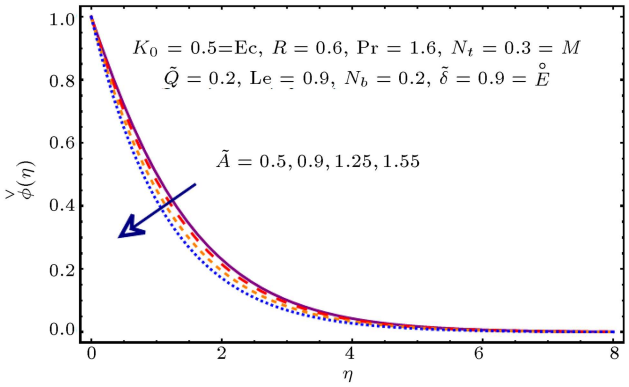

Figure 12. Impact on $\breve{\phi}(\eta)$ via $\tilde{A}$.

radiation respecting temperature. An increase of ($R = 0.2, 0.4, 0.6, 0.8$) enhances temperature. Here, the radiation parameter defines the transfer rate of thermal radiation relative to conductive heat transfer rate. At higher values of radiation parameter, the radiation term dominates over conduction. Hence, more heat releases in a system due to radiative heat flux and then, temperature increases. Figure 9 gives outcome of $\tilde{Q}$ with respect to temperature. Temperature increases as ($\tilde{Q} = 0.1, 1, 1.7, 2.4$) generates energy in the system. Outcomes of N_t and N_b with respect to concentration are given in Figures 10 and 11. The opposite trend is observed in case of higher ($N_t = 0.5, 0.9, 1.3, 1.7$) and ($N_b = 0.6, 0.9, 1.6, 2.7$) for concentration. Variation in the concentration of fluids against dimensionless chemical reaction parameter $\tilde{A}$ is given in Figure 12. An increase in ($\tilde{A} = 0.5, 0.9, 1.25, 1.55$) leads to a decrease in concentration. Figure 13 provides the impact of activation energy parameter ($\mathring{E}$) on concentration. According to the figure, the concentration rises for higher ($\mathring{E} = 0.2, 1.5, 2.1, 2.9$).

Effects of M and K_0 on $Re_x^{0.5}\tilde{C}_{fx}$ are shown in Figure 14. It is clear that $\mathrm{Re}_x^{0.5}\tilde{C}_{fx}$ increases for higher M and K_0. Figure 15 depicts the effects of Ec and R on $\mathrm{Re}_x^{-0.5}\tilde{N}_{ux}$. Higher values of R and Ec reduce

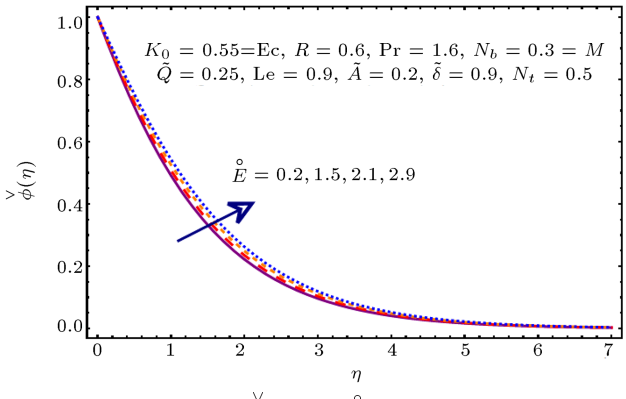

Figure 13. Impact on $\overset{\vee}{\varphi}(\eta)$ via $\overset{\circ}{E}$.

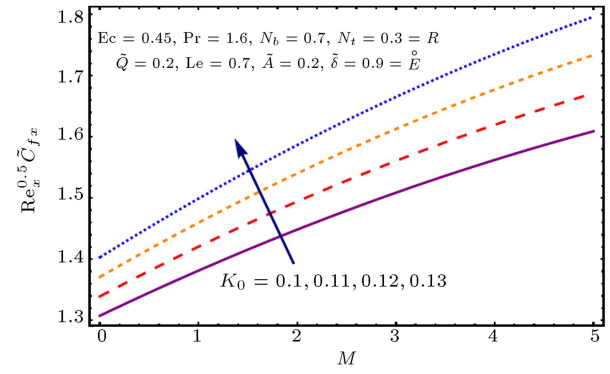

Figure 14. Impact of M and K_0 on $\mathrm{Re}_x^{0.5}\tilde{C}_{fx}$.

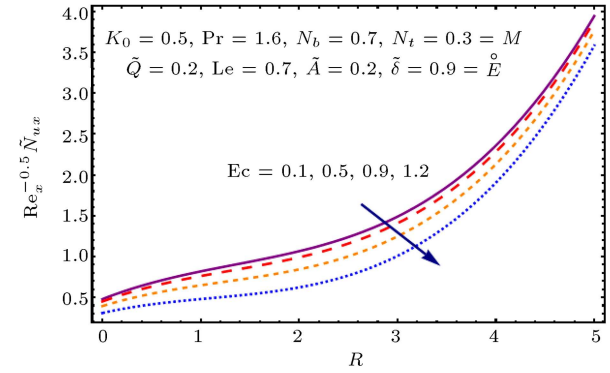

Figure 15. Impact of R and Ec on $\mathrm{Re}_x^{-0.5}\tilde{N}_{ux}$.

$\mathrm{Re}_x^{-0.5}\tilde{N}_{ux}$. Variations of $\overset{\circ}{E}$ and σ on $\mathrm{Re}_x^{-0.5}\tilde{S}_{hx}$ are shown in Figure 16. $(\mathrm{Re}_x^{-0.5}\tilde{S}_{hx})$ is the decreasing function of $\overset{\circ}{E}$ and $\tilde{A}$.

7. Entropy rate analysis

Figure 17 illustrates the outcome and effect of M on $N_G(\eta)$. Clearly, increases $N_G(\eta)$ for larger M. Consequences of Brinkman number Br on $N_G(\eta)$ are disclosed in Figure 18. $N_G(\eta)$ is enhanced by higher Br. In fact, irreversibility occurs for fluid friction by higher Br. Figure 19 indicates the effectiveness of K_0 in $N_G(\eta)$. An increase in $N_G(\eta)$ is noticed

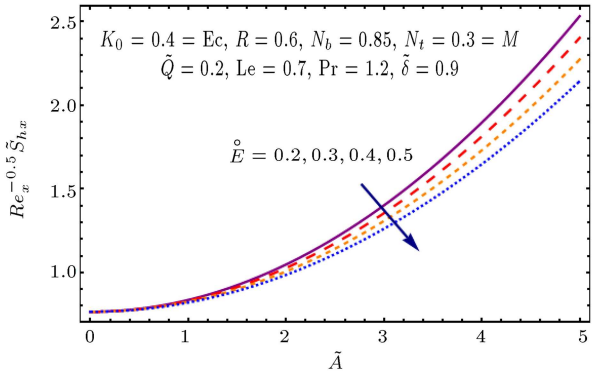

Figure 16. Impact of $\tilde{A}$ and $\overset{\circ}{E}$ on $\mathrm{Re}_x^{-0.5}\tilde{S}_{hx}$.

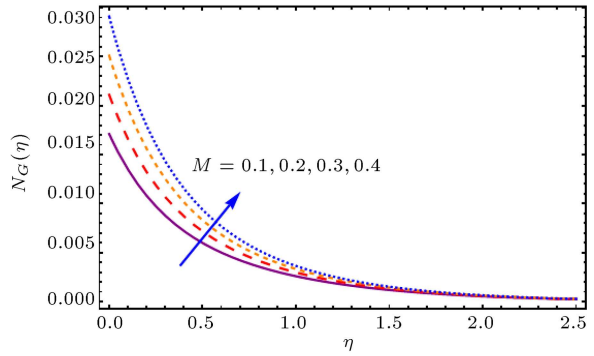

Figure 17. Impact of M on N_G.

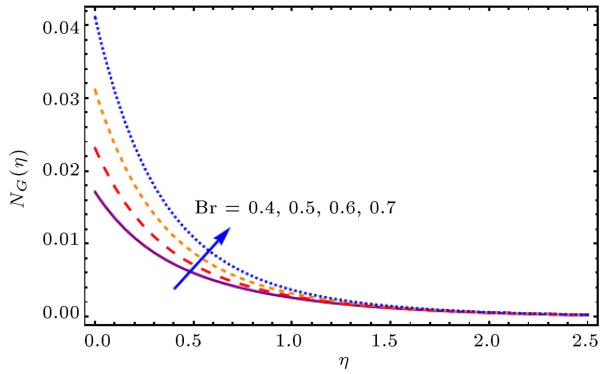

Figure 18. Impact of Br on N_G.

for K_0. Figure 20 presents the effect of temperature difference parameter ξ on $N_G(\eta)$. At higher ξ value, the entropy generation minimization accentuates, because heat transfer dominates over fluid friction and magnetic field for higher ξ.

8. Conclusions

Radiative nanofluid flow of Walters-B fluid under the effect of activation energy was investigated analytically. The significant effects of entropy rate and heat/generation absorption on the assumed simulations were observed and debated graphically. Remarkable highlights can be concluded as follows:

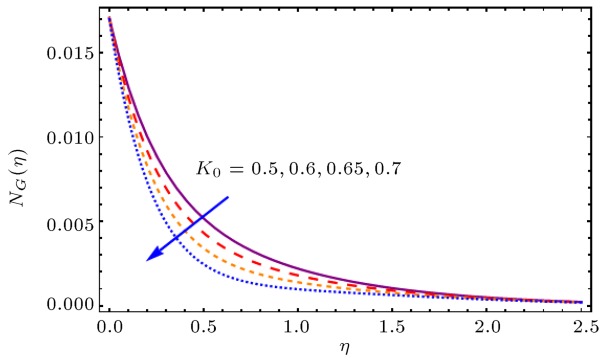

Figure 19. Impact of K_0 on N_G.

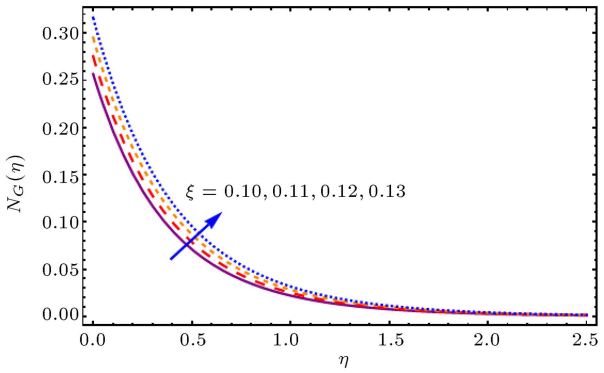

Figure 20. Impact of ξ on N_G.

- Qualitative effects of concentration and temperature were reversed for higher thermophoresis parameter;
- Temperature had a similar behavior for radiation and Eckert number;
- An enhancement of temperature was possible for heat/generation parameter;
- Concentration by an activation energy parameter increased;
- Decrease in mass transfer rate was noticed;
- Opposite behavior of total entropy rate for fluid parameter and temperature difference parameter was identified;
- Total entropy rate was an increasing function of Brinkman number and magnetic parameter.

References

1. Choi, S.U.S. "Enhancing thermal conductivity of fluids with nanoparticles", *ASME-Publications-Fed*, **231**, pp. 99–106 (1995).
2. Waini, I., Ishak, A., and Pop, I. "Hybrid nanofluid flow and heat transfer over a nonlinear permeable stretching/shrinking surface", Int. *J. Numerical Meth. Heat & Fluid Flow*, **29**(9), pp. 3110–3127 (2019).
3. Sheikholeslami, M. "Numerical approach for MHD Al_2O_3 -water nanofluid transportation inside a permeable medium using innovative computer method", *Comp. Meth. Appl. Mech. Eng.*, **344**, pp. 306–318 (2019).
4. Aly, E.H. "Dual exact solutions of graphene-water nanofluid flow over stretching/shrinking sheet with suction/injection and heat source/sink: Critical values and regions with stability", *Powder Tech.*, **342**, pp. 528–544 (2019).
5. Rafiq, T., Mustafa, M., and Khan J.A. "Numerical study of Bödewadt slip flow on a convectively heated porous disk in a nanofluid", *Phys. Scr.*, **94**(9), 095701 (2019).
6. Hsiao, K.L. "Micropolar nanofluid flow with MHD and viscous dissipation effects towards a stretching sheet with multimedia feature", Int. *J. Heat and Mass Transf.*, **112**, pp. 983–990 (2017).
7. Turkyilmazoglu, M. "MHD natural convection in saturated porous media with heat generation/absorption and thermal radiation: closed-form solutions", *Archi. Mech.*, **71**, pp. 49–64 (2019).
8. Ramzan, M., Bilal, M., and Chung, J.D. "Effects of thermal and solutal stratification on Jeffrey magneto-nanofluid along an inclined stretching cylinder with thermal radiation and heat generation/absorption", *Int. J. Mech. Sci.*, **132**, pp. 317–324 (2017).
9. Hsiao, K.L. "To promote radiation electrical MHD activation energy thermal extrusion manufacturing system efficiency by using Carreau-nanofluid with parameters control method", *Energy*, **130**, pp. 486–499 (2017).
10. Mustafa, M., Khan, J.A., Hayat, T., et al. "Buoyancy effects on the MHD nanofluid flow past a vertical surface with chemical reaction and activation energy", *Int. J. Heat and Mass Transf.*, **108**, pp. 1340–1346 (2017).
11. Hsiao, K.L. "Stagnation electrical MHD nanofluid mixed convection with slip boundary on a stretching sheet", *Appl. Therm. Eng.*, **98**, pp. 850–861 (2016).
12. Bejan, A. "A study of entropy generation in fundamental convective heat transfer", *ASME J. Heat Transfer*, **101**(4), pp. 718–725 (1979).
13. Bejan, A. and Kestin, J. "Entropy generation through heat and fluid flow", *J. Appl. Mech.*, **50**(2), p. 475 (1983).
14. Liu, Y., Jian, Y., and Tan, W. "Entropy generation of electromagnetohydrodynamic (EMHD) flow in a curved rectangular microchannel", *Int. J. Heat Mass Transf.*, **127**, pp. 901–913 (2018).
15. Qayyum, S., Khan, M.I., Hayat, T., et al. "Entropy generation in dissipative flow of Williamson fluid between two rotating disks", *Int. J. Heat Mass and Transf.*, **127**, pp. 933–942 (2018).
16. Akbarzadeh, M., Rashidi, S., and Karimi, N. "Convection of heat and thermodynamic irreversibilities in two-phase, turbulent nanofluid flows in solar heaters by corrugated absorber plates", *Adv. Powder Techn.*, **29**, pp. 2243–2254 (2018).

17. Bizhaem, H.K. and Abbassi, A. "Numerical study on heat transfer and entropy generation of developing laminar nanofluid flow in helical tube using two-phase mixture model", *Adv. Powder Techn.*, **28**(9) pp. 2110–2125 (2017).

18. Pal, S.K., Bhattacharyya, S., and Pop, I. "Effect of solid-to-fluid conductivity ratio on mixed convection and entropy generation of a nanofluid in a lid-driven enclosure with a thick wavy wall", *Int. J. Heat and Mass Transf.*, **127**, pp. 885–900 (2018).

19. Sheikholeslami, M. and Ganji, D.D. "Entropy generation of nanofluid in presence of magnetic field using lattice Boltzmann method", *Physica A*, **417**, pp. 273–286 (2015).

20. Wang, Y., Chen, Z., and Ling, X. "Entropy generation analysis of particle suspension induced by Couette flow", *Int. J. Heat Mass Transf.*, **90**, pp. 499–504 (2015).

21. Hayat, T., Khan, M.I., Qayyum, S., et al. "Entropy generation for flow of Sisko fluid due to rotating disk", *J. Mol. Liq.*, **264**, pp. 375–385 (2018).

22. Liao, S.J., *Homotopy Analysis Method in Non-linear Differential Equations*, Springer and Higher Education Press, Heidelberg (2012).

23. Noeiaghdam, S., Zarei, E., and Kelishami, H.B. "Homotopy analysis transform method for solving Abel's integral equations of the first kind", *Ain Shams Eng. J.*, **7**, pp. 483–495 (2016).

24. Hayat, T., Mustafa, M., and Asghar, S. "Unsteady flow with heat and mass transfer of a third grade fluid over a stretching surface in the presence of chemical reaction", *Nonlinear Analysis: Real World Appl.*, **11**(4), pp. 3186–3197 (2010).

25. Rahman, S., Hayat, T., Muneer, M., et al. "Global existence of solutions for MHD third grade flow equations saturating porous medium", *Comput. Math. Appl.*, **76**, pp. 2360–2374 (2018).

26. Jabeen, S., Hayat, T., Alsaedi, A., et al. "Consequences of activation energy and chemical reaction in radiative flow of tangent hyperbolic nanoliquid", *Scientia Iranica*, **26**(6), pp. 3928–3937 (2019). DOI: 10.24200/SCI.2019.52726.2860

27. Imtiaz, M., Kiran, A., Hayat, T., et al. "Axisymmetric flow by a rotating disk with Cattaneo-Christov heat flux", *J. Braz. Soc. Mec. Sci. Eng.*, **41**, p. 149 (2019).

28. Hayat, T., Ahmad, S., Khan, M.I., et al. "Modeling and analyzing flow of third grade nanofluid due to rotating stretchable disk with chemical reaction and heat source", *Physica B: Cond. Matt.*, **537**, pp. 116–126 (2018).

29. Abbasbandy, S. and Mustafa, M. "Analytical and numerical approaches for Falkner-Skan flow of MHD Maxwell fluid using a non-Fourier heat flux model", Int. *J. Num. Meth. Heat & Fluid Flow*, **28**, pp.1539–1555 (2018).

30. Turkyilmazoglu, M. "Convergence accelerating in the homotopy analysis method: a new approach", *Adv. Appl. Math. Mech.*, **10**, pp. 1–24 (2018).

31. Hayat, T., Qayyum, S., Khan, M.I., et al. "Entropy generation in magnetohydrodynamic radiative flow due to rotating disk in presence of viscous dissipation and Joule heating", *Phys. Fluids*, **30** p. 017101 (2018).

32. Qayyum, S., Hayat, T., and Jabeen, S. "Entropy generation in nanofluid flow of Walters-B fluid with homogeneous-heterogeneous reactions", *Math. Meth. Appl. Sci.*, pp. 1–16 (2020). https://doi.org/10.1002/mma.5997

33. Hsiao, K.L. "Combined electrical MHD heat transfer thermal extrusion system using Maxwell fluid with radiative and viscous dissipation effects", *Appl. Therm. Eng.*, **112**, pp. 1281–1288 (2017).

34. Turkyilmazoglu, M. "Multiple analytic solutions of heat and mass transfer of magnetohydrodynamic slip flow for two types of viscoelastic fluids over a stretching surface", *J. Heat Transfer*, **134**(7), p. 071701 (2012).

35. Turkyilmazoglu, M. "An effective approach for approximate analytical solutions of the damped Duffing equation", *Phy. Scrip.*, **86**(1), p. 015301 (2012).

Biographies

Sumaira Jabeen is a PhD student of Mathematics at Quaid-i-Azam University, Pakistan. She received his Master's degree from Quaid-i-Azam University. Her research interests are fluid mechanics, non-linear flow problems, and heat transfer.

Tasawar Hayat is a Pakistani Mathematician who has made pioneering research contributions to the area of mathematical fluid mechanics. He is considered one of the leading mathematicians working in Pakistan and currently is a Professor of Mathematics at the Quaid-i-Azam University.

Ahmad Alsaedi is a Professor at the Department of Mathematics at King Abdulaziz University, Jeddah, Saudi Arabia. He belongs to Nonlinear Analysis and Applied Mathematics (NAAM) research group. His area of interests includes fluid dynamics, nonlinear flow analysis, and flow problem in nanosystems.